The relationship between visual resolution and cone spacing in the human fovea

Ethan A. Rossi & Austin Roorda

Supplementary Information

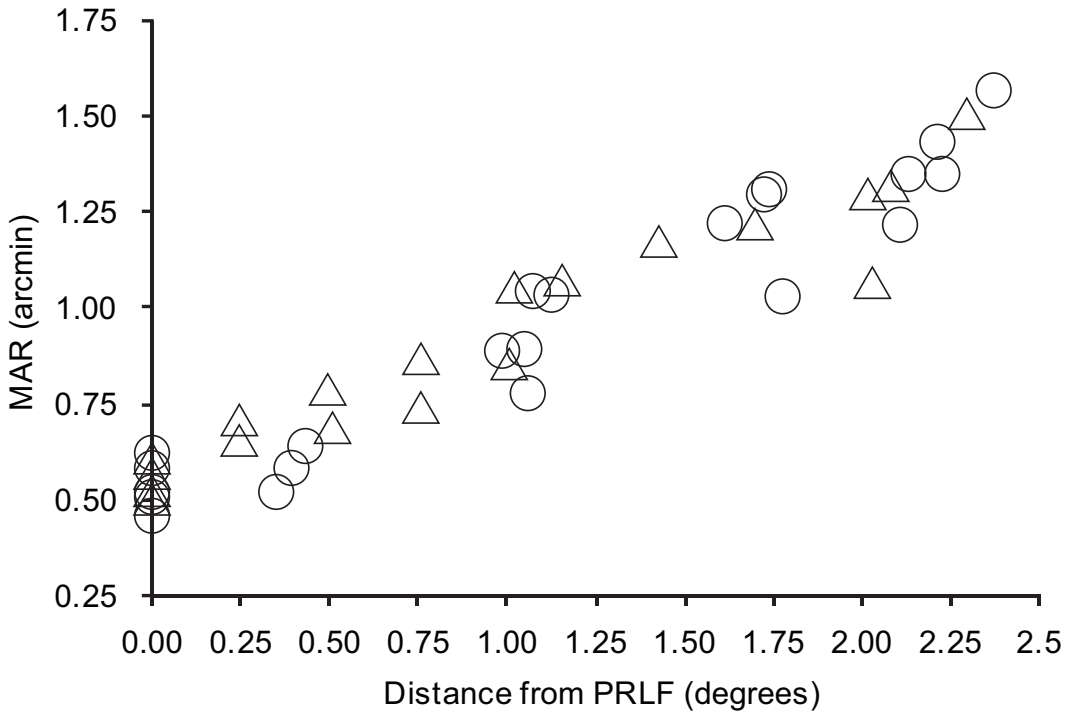

Supplementary Figure S1| **Tumbling E resolution measurements match results obtained with laser interferometry.** Interferometry results of Green[1] and Enoch & Hope[2] (triangles) are plotted with our measurements of MAR (circles). Results from Enoch & Hope[2] were converted from the reported "line pair separation" to an equivalent value of MAR, assuming that MAR was equal to the line pair separation (i.e. a line pair separation of 1 arcmin is equal to a MAR of 0.5 arcmin or a Snellen equivalent of 20/10).

Nature Neuroscience: doi:10.1038/nn.2465

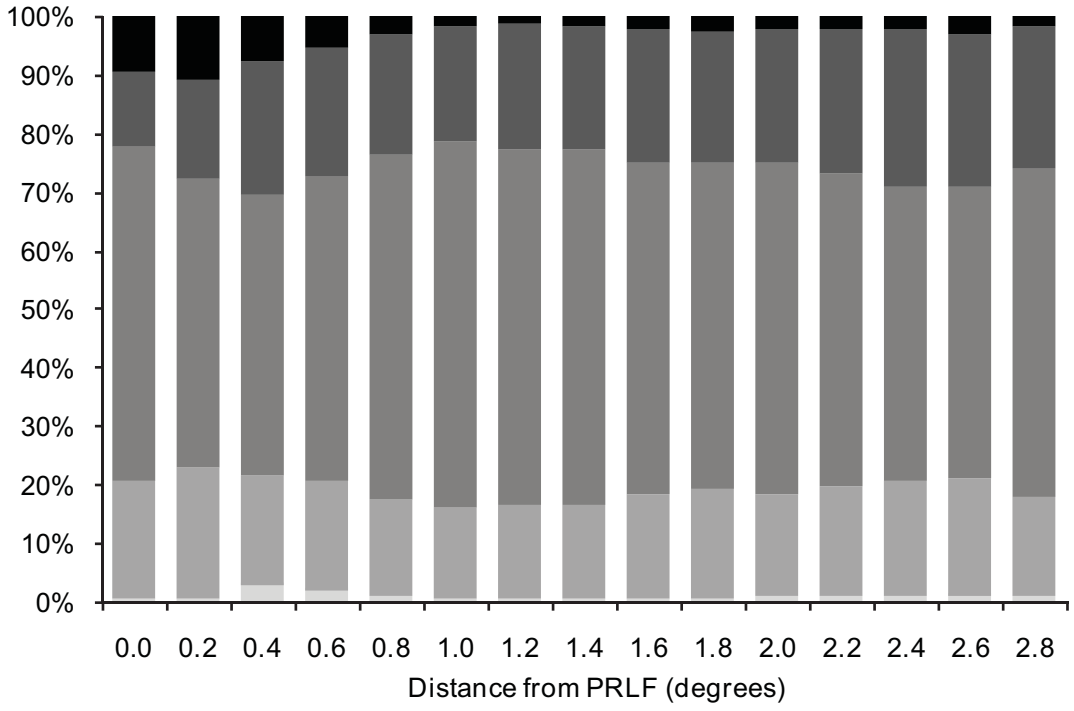

Supplementary Figure S2| **Mosaic regularity.** The regularity of the mosaic is plotted by showing the percentage of cones falling into different bins depending upon the number of neighbors. The stacked bar at each location is an average of more than one observer. Only two observers are averaged for the bars at 0, 0.2 and 2.8 degrees; four observers are averaged for the bars at 0.4 and 2.6 degrees; all 5 observers are averaged at all other locations. The number of cones having less than 4 neighbors is shown as the lightest grey level, with increasingly darker values representing 5, 6, or 7 neighbors, and with black representing more than 8 neighbors.

Nature Neuroscience: doi:10.1038/nn.2465

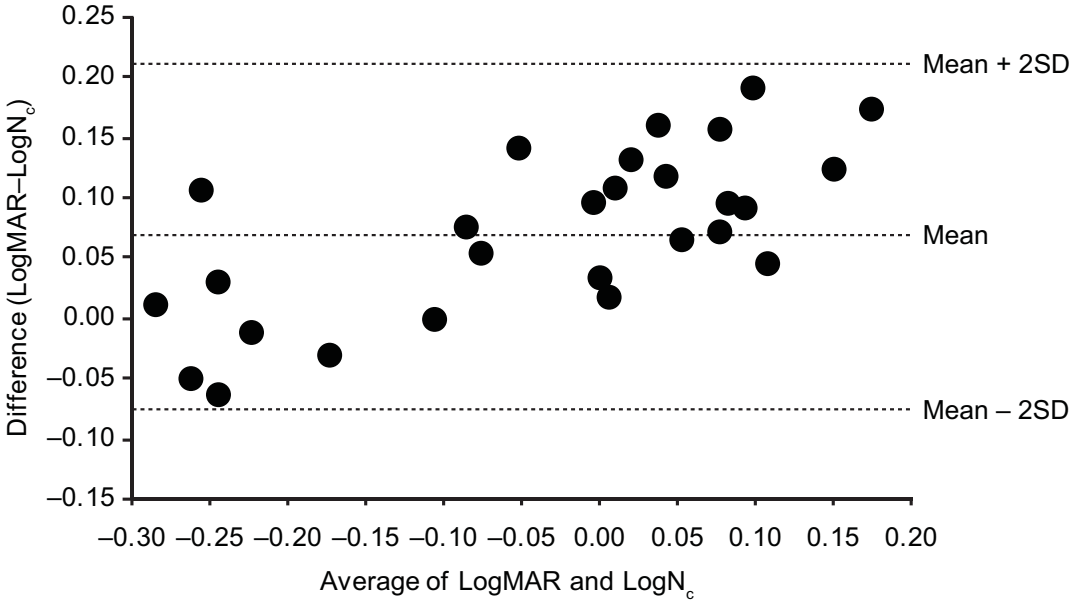

Supplementary Figure S3| **Bland-Altman plot shows poor agreement between MAR and N_c.** To assess the agreement between MAR and N_c, a Bland-Altman analysis was performed[13]. Bland-Altman analysis provides a simple and easy to interpret way for assessing agreement between two measurements[13]. Since the differences between MAR and N_c vary systematically across the range of measurement (i.e. the difference increases as MAR and N_c increase) and are proportional to the mean, a logarithmic transformation is appropriate[13] and has been performed. The Bland-Altman plot clearly illustrates that the difference between MAR and N_c can be quite large. The mean difference (bias) is 0.0679 on a log scale and the limits of agreement are –0.0766 and 0.2125. Taking the antilog of these limits gives 0.84 and 1.63; since the antilog of the difference between two values on a log scale is a dimensionless ratio[13], this shows that the values differ by between ~16% below and ~63% above, demonstrating poor agreement between MAR and N_c.

Nature Neuroscience: doi:10.1038/nn.2465

Supplementary Methods

Subjects. Two experienced observers (the authors; S1 & S2) and three naïve observers (S3–S5) with normal acuity and color vision participated in this experiment. Informed written consent was obtained in accordance with the procedures approved by the University of California, Berkeley Committee for the Protection of Human Subjects.

Apparatus and Stimuli. The AOSLO[10] and stimulus presentation method[12,16] are explained in detail elsewhere. Stimuli were presented in negative contrast (appearing as black on a red background). AO correction afforded a high contrast image at all test locations, with contrast increasing with stimulus size and thus eccentricity. Stimulus duration was 1 second (30 frames), exceeding the critical duration for optimal acuity at all test locations[17]. Retinal illumination was with a super luminescent diode laser (Superlum BroadLighter, S840-B-I-20); mean wavelength 840 nm and spectral FWHM of 50 nm. Field size was 48 arcmin (V) x 60 arcmin (H) for all locations and subjects except for the PRLF of S4 and S5 which was 24 arcmin (V) x 30 arcmin (H); retinal illuminance was ~2.1 and ~2.7 log Trolands for the two field sizes, respectively.

Procedure. Mydriasis and cycloplegia were induced with one drop of 2.5% phenylephrine and one drop of 1% tropicamide ~20 min prior to the start of the experimental session and were maintained throughout with an additional drop, if necessary. Head position was stabilized with a bite bar. Threshold estimation was performed by QUEST[18–19] and its implementation in AOSLO is explained elsewhere[12]. A few initial thresholds for subject S2 were determined after 100 trials; since the threshold changed little after ~40 trials, all subsequent measurements were obtained with 60 trial runs. This minimized experiment duration, observer fatigue and light exposure. Only two measurements were obtained for S5 at the most eccentric test location; all other thresholds shown are the average of 3–6 measurements.

Data Analysis. To build continuous maps of the retinal mosaic across all test locations, several videos were acquired prior to psychophysical testing. Videos were stabilized at 480 Hz (see example of a stabilized video in **Supplementary Video 2**) using custom algorithms[20] or at the frame rate (30 Hz) using custom written FFT-based methods in Matlab (The MathWorks, Natick, MA, USA). Stabilized videos were averaged to produce high signal to noise ratio images that were then combined into large montages manually in Photoshop (Adobe Systems, Inc., San Jose, CA, USA). The brightness and contrast of component images were adjusted to appear relatively the same in the large retinal montages. Sharp borders between overlapping component images in large montages were minimized using Photoshop. These large retinal mosaic images were then used to localize the center of each resolved cone using a combination of automated[21] and manual methods. The calculation of the size of retinal features and compensation for magnification effects due to spectacle lenses is explained in detail elsewhere[12]. To ease comparison with other published reports, N_c in **Fig. 2b** was calculated by determining center-to-center inter-cone distance (ICD) averaged over a 36.5 µm x 36.5 µm (1332.25 µm^2) sliding window from the PRLF which was then reduced by a factor of $\frac{\sqrt{3}}{2}$ to calculate N_c.

Nature Neuroscience: doi:10.1038/nn.2465

Identifying Stimulated Areas from AOSLO Videos. To find stimulated areas, each video of the stimulus on the retina was stabilized at the frame rate, resulting in a 30 Hz motion trace of eye position. All images from a given run were correlated using FFT based cross-correlation methods in Matlab and averaged to produce a high signal to noise ratio image of the stimulated area. The resulting image was then used as a proxy between the larger continuous retinal mosaic and the first frame of each individual trial video. This was done because single frames have a much lower signal to noise ratio than the high signal to noise ratio images of the retinal mosaic and correlating single frames with these images proved difficult. To relate each motion trace with the large retinal mosaics: 1) the location of the proxy image on the larger mosaic was determined and then 2) the location of the first frame on the proxy image was found. Both of these steps were accomplished using FFT based cross-correlations implemented in Matlab. Finally, the location of the stimulus on the first frame was found using the normalized two dimensional cross-correlation functions in Matlab. In this way the location of the stimulus at the beginning of each motion trace was localized on the larger mosaic. This location data, combined with the motion traces, stimulus sizes, and cone spacing parameters allowed for cone interactions to be modeled (as explained below). For most observers, motion traces were computed for all thirty frames. A delay between stimulus presentation and recording occurred for two observers (S4 & S5), which resulted in just the final 21–23 frames being available for motion analysis. Some videos from all observers were excluded due to poor quality of the retinal imagery, blinks, or large eye movements. Of 7580 total trials for all observers, 93.7% were successfully analyzed and localized on the retinal imagery. This data was used to calculate the mean position stimulated at each test location, in addition to a standard deviation in both the x and y directions. These values were used to define an elliptical area in which the stimulus fell at each test location, over which N_c was averaged for comparison to MAR in **Fig. 2c**.

Calculation of Cone Stimulation Maps. To accurately determine cone-stimulus interactions, we used our cone position and spacing data to create a simple model in Matlab of the spatial sampling characteristics of the cone mosaic. Each cone has an associated aperture whose size is based upon the spacing between a cone and all of its neighbors. The shape of the aperture is assumed to be Gaussian with full width at half maximum of 34% of ICD[22]. In this way, a digital two dimensional model of the cone apertures is created. To examine the interaction of the stimulus with the model of cone apertures, a model of the light distribution on the retina is also computationally created. This is done by convolving the point spread function due to diffraction at 840 nm with the light distribution of the stimulus. The retinal model is then multiplied by the stimulus model and the result is an estimate of the pattern of cone stimulation at the level of the cones. To calculate cone stimulation maps, for each trial the stimulus was scaled appropriately based upon the actual stimulus that was delivered to the retina. Using the motion information and location of the calculated frame rate traces, the motion during each trial was simulated and the pattern of cone interactions estimated for each frame. For each cone, the light distribution was integrated across the entire cone aperture. This value was then normalized to the degree to which the aperture was filled. If the entire aperture is filled, that cones stimulation was considered to be maximal. In this way cone stimulation maps were created, showing which cones were stimulated over the course of a trial. This process is illustrated in **Supplementary Video 3**.

Nature Neuroscience: doi:10.1038/nn.2465

Mosaic Regularity. Mosaic regularity was assessed with several simple geometric methods. All assessments were based on the locations of cone centers identified from retinal imagery that were then triangulated using the Delaunay triangulation implemented in Matlab. Since we are concerned with looking at how regular the mosaic is over the areas stimulated during acuity tests, we used a larger averaging window for assessing regularity in the mosaic than we did for calculating spacing for **Fig. 2b**. The averaging window for mosaic regularity assessment was 85 μm x 85 μm, or roughly 17.4 arcmin, which is ≅ ± 2SD of the mean eye position for all observers. Delaunay triangulation allowed for the x,y position of each neighbor of each cone to be found. At each location where cones were well resolved, the average number of neighbors was 6 (SD = 0.7), and the average angle between cones was ~60° (SD = 7.5). Another way to consider the regularity of the mosaic is to compare the percentage of cones having six neighbors to those having more or fewer neighbors. This is shown in **Fig. S3**, averaged for all observers across the temporal horizontal retina (see figure legend for **Fig. S3**). On average, most cones have six neighbors (50–60%), the majority of the rest have 5 or 7 (~15–20% each), and only a small percentage have fewer than four or more than eight neighbors. This indicates that there was indeed a regular triangular lattice of cone photoreceptors across test locations, in agreement with findings for normal human fovea. [21,23]

Estimating Cone Spacing at the Foveal Center. This was accomplished by simple linear regression analysis of the points between where cones became well resolved and ~400 μm from the PRLF. It has been shown that the reduction in cone spacing within this area is approximately linear[9]. We used the data of Curcio[9] to test this method and found that using the published measurements for the temporal fovea between 150 μm (~0.5º) and 400 μm (~1.4º) to predict N_c at the foveal center results in an RMS error of ~0.043 arcmin. Using more data improves the estimate slightly; using the published measurements between 100 μm (~0.35º) and 400 μm (~1.4º) results in an RMS error of ~0.041 arcmin. Decreasing the number of points (using only those between 200 μm and 400 μm) results in an RMS error of 0.054 arcmin. For one observer, S4, estimates were taken from the data points at eccentricities between 0.7º and 1.4º. We therefore expect our estimates of spacing at the PRLF to be accurate to within ~± 0.05 arcmin.

Calculation of mRGC receptive field spacing. The model of midget ganglion cell receptive field density (D_{mgcrf}) in the human visual field from Drasdo and colleagues was used to estimate the Nyquist limit of midget retinal ganglion cell receptive fields (N_{mRGC}). Using equation 6 from Drasdo et al.[15], we calculated D_{mgcrf} at the test eccentricities for our observers. Parameter values for their general model were used. By dividing D_{mgcrf} by two at all locations we were able to estimate the density of either the ON- or OFF-center subclass of mRGCs. For our purposes we assume that the ON- and OFF-center sub mosaics are symmetric and tile the visual field completely at our foveal test locations. It has been suggested that there is considerable asymmetry in the ON and OFF mRGC mosaics in the periphery, but this has not been demonstrated within 5º from the foveal center[7]. Density is converted to spacing between rows of ON- or OFF-center mRGC receptive fields using the following equation:

Nature Neuroscience: doi:10.1038/nn.2465

$$N_{mRGC} = \sqrt{\frac{\sqrt{3}}{2 \times D_{mgcrf}}}$$

This conversion assumes that the mRGC receptive fields tile the visual field in a triangular packing arrangement, in the same way as the cone photoreceptors. The value of E_2 for N_{mRGC} (the eccentricity at which spacing between ON- or OFF- mRGC receptive field centers doubles) predicted from the model of Drasdo and colleagues[15] is 1.209º, similar the mean obtained for E_{2m} (~1.275°).

Supplementary Discussion

Comparison of results to previous psychophysical studies. As already noted, the MAR results obtained in this study are in close agreement with the studies of Green[1] and Enoch & Hope[2] who used laser interferometry to measure resolution across the range of test locations examined here (0–2.5°) (**Fig. S1**). Laser interferometry effectively bypasses the normal optics of the eye, allowing for resolution measurements to be obtained that are free from the limitations imposed by the normal optics of the eye[1–4]. If our resolution measurements were worse than those obtained by laser interferometry, the discord seen between our resolution results and N_c measurements could be due to the retinal illuminance of our stimulus, which is beyond the level where grating resolution is believed to be independent of illuminance, but slightly below the level where Landolt C resolution is believed to be optimal[24]. However, the fact that our resolution measurements are in such good agreement with those obtained using bright high contrast laser interference fringes shows that a stimulus based explanation for the difference found between N_c and MAR is highly unlikely. Furthermore, the mean MAR obtained at the PRLF of 0.544 arcmin (n = 5) is nearly identical to the average MAR of 0.537 arcmin (n = 20) from a previous study in this laboratory, obtained with the same instrument and experimental protocol, but with a wavelength of 658 nm and retinal illuminance of 6.8 log Trolands[12].

The results of Green[1] and Enoch & Hope[2] diverge from each other beyond our range of testing, with the two observers in the Enoch & Hope study achieving better resolution (lower equivalent MAR) at eccentricities beyond ~3° from the PRLF[2]. Both studies used estimates of cone spacing from the classic study of Østerberg[25] for comparison and drew different conclusions. It should be noted that the peak cone density reported by Østerberg[25] at the foveal center was lower than 6 of the 8 eyes examined by Curcio and was more than one SD unit lower than Curcio's mean of 8 eyes between 0.15 mm and 1 mm (~0.5° to ~3.5°) [9]; lower cone density results in higher estimates of cone spacing. Because the results of observer JE fell along the estimates of cone spacing from Østerberg[25] out to the most eccentric location tested (7°), Enoch & Hope concluded that resolution and cone spacing agreed over this range[2]. However, Green's observers diverged from the spacing measurements of Østerberg[25] at around 2 degrees[1] so they came to a different conclusion. This discrepancy is likely to be partially accounted for in differences in methodology, and in particular the size of the test field[2]. Enoch & Hope showed that using a small test field (17 arcmin versus 44 arcmin) reduced performance; resolution was better with the larger test field[2]. However, the fact remains that there is a large discrepancy in results outside the anatomical fovea.

Nature Neuroscience: doi:10.1038/nn.2465

More recently, the region of equivalence between N_c and visual resolution has been shown to persist over a greater range, out to about 10° from the center of the fovea. Both Williams & Coletta[3] and Thibos et al.[4] also used interference fringes to test vision over a range of retinal eccentricities. Using the method of adjustment, Thibos found resolution agreed with spacing measurements derived from the Østerberg[25] report out to ~10° from the foveal center[4]. In a second experiment from the same report, Thibos et al. also employed a detection task, whereby observers "reduced spatial frequency until the presence of spatial contrast was evident"[4]. With this task, they showed that gratings above the Nyquist limit could be *detected* (or at least contrast could be detected, as Thibos et al. note that "there was no requirement that the percept be of a grating") when the spatial frequency was much higher than N_c and also of the Nyquist limit of the RGCs to which he compared his measurements[4].

A similar finding was made by Williams & Coletta[3]. However, they had previously obtained psychophysical estimates of the Nyquist limit of the cone mosaic of their observers[26] and so were the first researchers that were able to compare resolution measurements directly to estimates of the Nyquist limit from the same observers. Their estimates of the Nyquist limit were in reasonable agreement with Østerberg[25] and Curcio's[27] measurements, but their resolution measurements were much better than predicted by the Nyquist limit of the cone mosaic, with their observers able to guess the correct orientation of the grating (either horizontal or vertical) when it was ~1.5 times the Nyquist limit[3]. In a separate experiment in the same report, Williams and Coletta also employed a forced-choice orientation discrimination task to measure contrast sensitivity for a range of spatial frequencies at 3.8º and stated that their results "provide no support for the notion that postreceptoral mechanisms restrict visual resolution to values below the cone Nyquist frequency".[3] They showed that supra-Nyquist performance persisted to ~10º, and only at their next test location (20º) did performance finally fall below the Nyquist limit. They conclude: "thus the present data support the generally held belief that, beyond 10 deg at least, the limitations on visual resolution in the peripheral retina are mainly postreceptoral". [3] It should be noted that the results of Williams & Coletta[3] and Thibos et al.[4] are supported by evidence from macaque which suggests monkey acuities are in close agreement with cone Nyquist frequencies out to ~10° and ganglion cell Nyquist limits beyond[28].

The field size used for the resolution measurements made by Thibos et al.[4] and Williams and Coletta[3] were larger than those used by either Green[1] or Enoch & Hope[2]. The field size employed by Thibos et al. was 2.5° in diameter at the 5° eccentric test location, and 3° in diameter all other locations[4]. As was shown by Enoch & Hope, increasing the size of the test field can improve resolution[2]. Increasing field size increases both the number of cycles of the grating that are visible, as well as the length of the fringes[2] but also (and possibly more importantly) results in a larger area of retinal stimulation. This introduces the possibility that observers may use the edges of the stimulus closer to the foveal center, which falls on cones that are more closely spaced than on the more eccentric edge of the field, to make their determination[2,3]. For example, the smallest test field used by Thibos et al.[4] (2.5° in diameter), at the eccentricity of 5° would stimulate a retinal area (if fixation was perfect) extending from 3.75º–6.25º. Cone spacing increases rapidly in this area, from ~1.6 to ~2 arcmin in the data of Østerberg[25], an increase in spacing of ~25%, making the comparison here

Nature Neuroscience: doi:10.1038/nn.2465

subject to a considerable amount of error. Field sizes used by Williams & Coletta[3] were progressively larger at each retinal area, scaled to be ~80 times the cone spacing (as measured by Østerberg[24]) at each eccentricity[3]. It is possible that some of the supra Nyquist performance was therefore due to the larger field sizes stimulating areas closer to the foveal center, however, as noted by Williams & Coletta, this hypothesis does not account for much of the discrepancy found between resolution and the Nyquist limit of the cone mosaic[3].

Clearly the different tasks employed in these studies utilize different mechanisms, as is evidenced by their drastically different visual thresholds. Williams and Coletta offer an aliasing hypothesis as one possible explanation for the supra Nyquist resolution observed in their study: since aliasing noise below twice the Nyquist frequency is slightly anisotropic, the correct orientation of the grating may be determined even if the signal from the grating alone was too weak for the observer to properly guess the orientation[3]. We believe that the aliasing hypothesis provides some explanation for supra Nyquist performance. Furthermore, Williams and Coletta state that: "the sampling theorem correctly specifies the highest frequency possible for image reconstruction without aliasing. However, it does not necessarily prevent an observer from extracting enough critical features of a supra-Nyquist grating to be confident that he sees it".[3] We believe that this statement points to an explanation that may explain the differences seen between our data and those of Thibos et al.[4] and Williams & Coletta[3].

Although we have shown that the model of Drasdo and colleagues[15] suggests that there is on average fewer than 2 cones per mRGC outside the foveal center, and thus we have argued that this circuitry suggests that resolution should no longer match N_c, it has been shown that there exist mRGCs at eccentricities well beyond the foveola (at ~7°) which connect to single cones[29]. Logic dictates that although one, two or more cones may connect to an ON- or OFF-center mRGC, a fraction of a cone cannot (ie. 1.5 cones). That is not to say that an ON- or OFF-center mRGC cannot be driven primarily by a single cone, with weak input coming from one or more surrounding cones, in fact this has been shown to be the case in the retina of macaque[30–31]. However, the Drasdo et al. model[15] clearly suggests a smooth transition (on average) from single cone centers in the foveola to multi-cone centers in the periphery. For this relationship to exist there must be a fraction of mRGC receptive fields that are driven primarily by single cone input to the center of their receptive fields out to at least the eccentricity where the average rises to 2 cones per mRGC and perhaps beyond. As eccentricity increases, the proportion of single cone center mRGCs decreases, while the proportion having multiple cone centers increases. Information provided by single cone center mRGCs at eccentric locations may thus provide the visual system with enough information about the critical features of the grating stimulus for an observer to correctly specify the orientation. This could also explain the reduction in MAR seen with increased field size, as a larger field would presumably encounter more single cone centered mRGCs (due to the larger area stimulated) and thus provide a stronger signal to the orientation or presence of the grating than would a smaller field.

The final psychophysical study we feel it is important to discuss herein is that of Marcos and Navarro[5]. This is only other study that we know of (aside from the present one) that compared objectively measured cone spacing and visual performance in the same eyes. The major drawback of this study that prevents direct comparison to our

Nature Neuroscience: doi:10.1038/nn.2465

results is that they measured visual performance through the normal optics of the eye. Their main finding was that visual acuity matched the Nyquist limit of the cone mosaic across the fovea (they tested only from 0–1°), except at the precise foveal center, where optical aberrations were the limiting factor[5]; this finding is in agreement with the other studies considered[1–4]. Although it is shown in Figure 7 of their study that all four of their observers performed worse than the Nyquist limit of the cone mosaic at their most eccentric test location of 1º, it is mentioned only briefly in the text, and in that case regarding the significance with respect to one observer. It appears that the difference was therefore not significant for the other 3 observers, although there appears to clearly be a trend toward underperformance at 1° from the foveal center. However, since the optical aberrations of eye were uncorrected, it is impossible to rule out whether optical factors were still limiting performance to some extent at this location, as Green[1] showed optical factors to be a limiting factor out to an eccentricity of ~5°.

Supplementary References

16. Poonja, S., Patel, S., Henry, L. & Roorda, A. *J. Refract. Surg.* **21(5)**, S575–S580 (2005).
17. Baron, W.S. & Westheimer, G. *J. Opt. Soc. Am.* **63(2)**, 212–219 (1973).
18. Watson, A.B., & Pelli, D.G. *Percept. Psychophys.* **33(2)**, 113–120 (1983).
19. Pelli, D.G. *Spat. Vis.* **10(4)**, 437–442 (1997).
20. Arathorn, D.W. *et al. Opt. Express* **15(21)**, 13731–13744 (2007).
21. Li, K.Y. & Roorda, A. *J. Opt. Soc. Am. A* **24(5)**, 1358–1363 (2007).
22. Williams, D., Sekiguchi, N., & Brainard, D. *Proc. Natl. Acad. Sci. USA* **90**, 9770–9777 (1993).
23. Curcio, C.A. & Sloan, K.R. *Vis. Neurosci.* **9(2)**, 169–180 (1992).
24. Shlaer, S. *J. Gen. Physiol.* **21**, 165–188 (1937).
25. Østerberg, G.A. *Acta Opthalmol.* **13**(Suppl. 6): 1–102 (1935).
26. Coletta, N.J. & Williams, D.R. *J. Opt. Soc. Am. A* **4(8)**, 1503–1513 (1987).
27. Curcio, C.A., Sloan, K.R. Jr., Packer, O., Hendrickson, A.E. & Kalina, R.E. *Science* **236(4801)**, 579–582 (1987).
28. Merigan, W.H. & Katz, L.M. *Vision Res.* **30**(7), 985–991 (1990).
29. Kolb, H. & Marshak, D. *Doc. Ophthal.* **106**, 67–81 (2003).
30. McMahon, M.J., Lankheet, M.J.M., Lennie, P., & Williams, D.R. *J. Neurosci.* **20**(5), 2043–2053 (2000).
31. Sincich, L.C., Zhang, Y., Tiruveedhula, P., Horton, J.C., & Roorda, A. *Nature Neurosci.* **12**, 967–969 (2009).

Nature Neuroscience: doi:10.1038/nn.2465

Supplementary Video Legends

Supplementary Video 1| **AOSLO video showing retinal imagery and stimulus delivery.** This video shows a tumbling E stimulus being delivered to the retina of observer S3. Cone photoreceptors appear as bright circles arranged in a roughly triangular lattice pattern. The motion of the retinal mosaic is due to normal fixational eye movements. This video has been processed in the following way: sinusoidal distortion caused by raster scanning was removed[10,12,16]; the aspect ratio was corrected to be 1:1; the video was cropped to be 0.75° x 0.75°. Although the stimulus appears quite sharp, this is due to the fact that the stimulus is delivered by modulating the imaging beam to be off. What the observer sees is a stimulus that is blurred by diffraction and any residual high-order optical aberrations that exist after AO correction.

Supplementary Video 2| **Stabilized AOSLO video.** Video 2 shows a stabilized version of video 1. This video was stabilized using custom algorithms[20] and illustrates how the normal fixational movements of the eye cause the stimulus to move across several photoreceptors over the course of a one second trial (30 frames). Stabilized videos such as these were averaged to produce the high signal to noise ratio images images which were used to build continuous maps of the photoreceptor mosaic for all individuals across test locations. Motion traces obtained through stabilization were used to determine the precise location of stimuli presented to the retina for resolution testing and for creating stimulation maps such as the one shown in **Fig. 1**.

Supplementary Video 3| **Animation showing modeled cone-stimulus interaction.** This animation illustrates how cone models were used to examine the interaction between the stimulus and photoreceptor mosaic. This video shows the cone-stimulus interaction that occurred during the trial shown in videos 1 & 2. This animation only shows a subsection of the area shown in videos 1 and 2; scale bar shows size relations. The left panel shows how the convolved stimulus moved across the cone mosaic, while the right panel shows the simulated cone interactions. The stimulus edges are enhanced (brightened) in the left panel to clearly illustrate where the contrast in the image fell to 50% of maximum. The color bar indicates the relative level of stimulation integrated over the course of the presentation for each cone. The change in color from blue to red as cones are stimulated over the course of the presentation illustrates how cone stimulation maps such as figure 1 were created.

Nature Neuroscience: doi:10.1038/nn.2465